Molecular Orientation-Dependent Ionization Potential of Organic Thin Films

Wei Chen,* Han Huang, Shi Chen, Yu Li Huang, Xing Yu Gao, and Andrew Thye Shen Wee*

Department of Physics, National University of Singapore, 2 Science Drive 3, 117542, Singapore

Received June 17, 2008. Revised Manuscript Received September 30, 2008

Orientation-dependent ionization potentials (IPs) of organic thin films have been investigated with the combination of synchrotron-based high-resolution photoemission spectroscopy and near-edge X-ray absorption fine structure measurements. Organic thin films of copper(II) phthalocyanine (CuPc) and its fully fluorinated counterpart of copper hexadecafluorophthalocyanine (F_{16}CuPc) with well-controlled orientation are used as model systems. Both molecules lie flat on the graphite surface and stand upright on Au(111) terminated by self-assembled monolayer of octane-1-thiol. The IP for the standing-up CuPc thin film (IP = 4.75 eV) is 0.40 eV lower than that of the lying-down film (IP = 5.15 eV). In contrast, the IP of the standing up F_{16}CuPc (IP = 6.50 eV) is 0.85 eV higher than that of the lying-down film (IP = 5.65 eV). This reversed orientation dependence in IP is explained by the opposite surface dipoles in the standing-up CuPc and F_{16}CuPc molecular layers originating from the different intramolecular dipolar bonds exposed at the surfaces, i.e., a net upward pointing surface dipole in the standing-up CuPc thin film that lowers the IP, and a net downward pointing surface dipole in the standing-up F_{16}CuPc thin film that increases the IP.

Introduction

Organic semiconducting thin films comprising π-conjugated organic molecules usually possess highly anisotropic properties, such as light absorption and charge transport, which largely depend on the supramolecular packing and molecular orientation of the films.[1,2] Much research has been devoted to the manipulation of molecular packing and orientation, in particular to control the film properties for applications in organic based devices such as organic solar cells, organic thin film transistors, organic light-emitting diodes and organic spintronics. For example, studies have been done on aligning the molecular $\pi-\pi$ stacking of organic thin films along the charge transport direction to achieve higher charge carrier mobilities,[1−3] controlling the molecular orientation for efficient light absorption,[4−6] manipulating the polymorphism or supramolecular packing structures to realize magnetic switch in organic thin films,[7] and so on.

Recently, orientation-dependent ionization potentials (IPs) of organic thin films have been reported,[8−15] where IP refers to the energy difference between the highest-occupied-molecular-oribital (HOMO) and the vacuum level (E_{vac}).[16] Large variations in IPs up to 0.6 eV have been observed for α,ω-dihexyl-sexithiophene (DH6T) and α-sexithiophene (6T) films on Ag(111), depending on whether the molecules are lying flat on the substrates or standing upright.[8] Duhm et al. attributed the observed orientation dependence of IP in 6T and DH6T thin films on Ag(111) to the different surface dipoles built into the molecular layers.[8] Therefore, manipulation of IP via controlling the molecular orientation in organic thin films could be an effective way to reduce the charge injection barriers in organic electronic devices.

* Corresponding author. E-mail: phycw@nus.edu.sg (W.C.); phyweets@nus.edu.sg (A.T.S.W.).

(1) Dimitrakopoulos, C. D.; Malenfant, P. R. L. *Adv. Mater.* **2002**, *14*, 99.
(2) Coropceanu, V.; Cornil, J.; da Silva, D. A.; Olivier, Y.; Silbey, R.; Bredas, J. *Chem. Rev.* **2007**, *107*, 926.
(3) Garnier, F.; Yasser, A.; Hajlaui, R.; Horowitz, G.; Deloffre, F.; Servet, B.; Ries, S.; Alnot, P. *J. Am. Chem. Soc.* **1993**, *115*, 8716.
(4) Sylvester-Hvid, K. O. *J. Phys. Chem. B.* **2006**, *110*, 2618.
(5) de Bettignies, V.; Nicolas, Y.; Blanchard, P.; Levillain, E.; Nunzi, J.-M.; Roncali, J. *Adv. Mater.* **2003**, *15*, 1939.
(6) Videlot, C.; El Kassmi, A.; Fichou, D. *Sol. Energy. Mater. Sol. Cells* **2000**, *63*, 69.
(7) Heutz, S.; Mitra, C.; Wu, W.; Fisher, A. J.; Kerridge, A.; Stoneham, M.; Harker, T. H.; Gardener, J.; Tseng, H.-H.; Jones, T. S.; Renner, C.; Aeppli, G. *Adv. Mater.* **2007**, *19*, 3618.
(8) Duhm, S.; Heimel, G.; Salzmann, I.; Glowatzkl, H.; Johnson, R. L.; Vollmer, A.; Rabe, J. P.; Koch, N. *Nat. Mater.* **2008**, *7*, 326.
(9) Koch, N.; Salzmann, I.; Johnson, R. L.; Pflaum, J.; Friedlein, R.; Rabe, J. P. *Org. Electron.* **2006**, *7*, 537.
(10) Fukagawa, H.; Yamane, H.; Kataoka, T.; Kera, S.; Nakamura, M.; Kudo, K.; Ueno, N. *Phys. Rev. B.* **2006**, *73*, 245310.
(11) Friedlein, R.; Crispin, X.; Pickholz, M.; Keil, M.; Stafstrom, S.; Salaneck, W. R. *Chem. Phys. Lett.* **2002**, *354*, 389.
(12) (a) Ivanco, J.; Winter, B.; Netzer, T. R.; Ramsey, M. G. *Adv. Mater.* **2003**, *15*, 1812. (b) Ivanco, J.; Netzer, F. P.; Ramsey, M. G. *J. Appl. Phys.* **2007**, *101*, 103712. (c) Ivanco, J.; Haber, T.; Krenn, J. R.; Netzer, F. P.; Resel, R.; Ramsey, M. G. *Surf. Sci.* **2007**, *601*, 178.
(13) Ihm, K.; Kim, B.; Kang, T.-H.; Kim, K.-J.; Joo, M. H.; Kim, T. H.; Yoon, S. S.; Chung, S. *Appl. Phys. Lett.* **2006**, *89*, 033504.
(14) Salzmann, I.; Duhm, S.; Heimel, G.; Oehzelt, M.; Kniprath, R.; Johnson, R. L.; Rabe, J. P.; Koch, N. *J. Am. Chem. Soc.* **2008**, *130*, 12870.
(15) Yamane, H.; Yabuuchi, Y.; Fukagawa, H.; Kera, S.; Okudaira, K. K.; Ueno, N. *J. App. Phys.* **2006**, *99*, 093705.
(16) (a) Ishii, H.; Sugiyama, K.; Ito, E.; Seki, K. *Adv. Mater.* **1999**, *11*, 605. (b) Kahn, A.; Koch, N.; Gao, W. Y. *J. Polymer. Sci. B.* **2003**, *41*, 2529. (c) Cahen, C.; Kahn, A. *Adv. Mater. Adv. Mater.* **2003**, *15*, 271. (d) Koch, N. *ChemPhysChem.* **2007**, *8*, 1438. (e) Tang, J. X.; Lee, C. S.; Lee, S. T. *J. Appl. Phys.* **2007**, *101*, 064504.

10.1021/cm8016352 CCC: $40.75
Published on Web 10/29/2008

In contrast to organic molecules on reactive semiconductors with unsaturated dangling bonds,[17] on chemically inert and atomically flat substrates such as graphite, single crystal metals and SiO_2, the molecular orientation in organic thin films is largely determined by the balance between molecule−substrate interfacial and intermolecular interactions.[18−27] For example, on graphite, planar copper(II) phthalocyanine (CuPc) lies flat on the surface, stabilized by the interfacial dispersion force;[28] on Au(111), CuPc also adopts the flat-lying configuration because of the effective coupling between the metal d-bands and conjugated π system (d−π interaction).[29] On the other hand, by terminating the Au(111) surface with various self-assembled monolayers (SAMs) of aromatic thiols, the d−π interface interaction is minimized, thereby leading to a standing-up configuration of CuPc on SAMs/Au(111).[30] In this article, we use synchrotron-based photoemission spectroscopy (PES) and near-edge X-ray absorption fine structure (NEXAFS) measurements to study the orientation dependent IP of both lying-down and standing-up organic thin films of CuPc and its fully fluorinated counterpart of copper hexadecafluorophthalocyanine (F_{16}CuPc). The combination of these two organic materials has promising applications in ambipolar organic field-effect transistors.[31] We observe reversed orientation dependence of IP in both films, i.e., the IP for the standing-up CuPc is lower than that of the lying-down CuPc, whereas the IP for the standing-up F_{16}CuPc is higher than that of lying-down F_{16}CuPc. Such reversed orientation dependence in the IPs is explained by the opposite surface dipoles induced in the standing-up CuPc and F_{16}CuPc molecular layers.

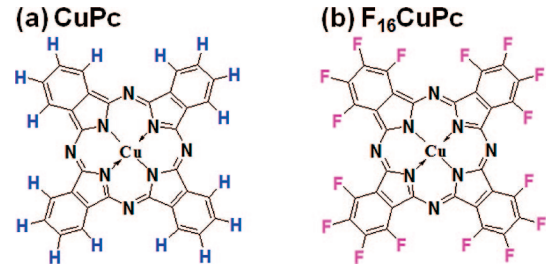

Figure 1. Schematic drawings for (a) CuPc and (b) F_{16}CuPc.

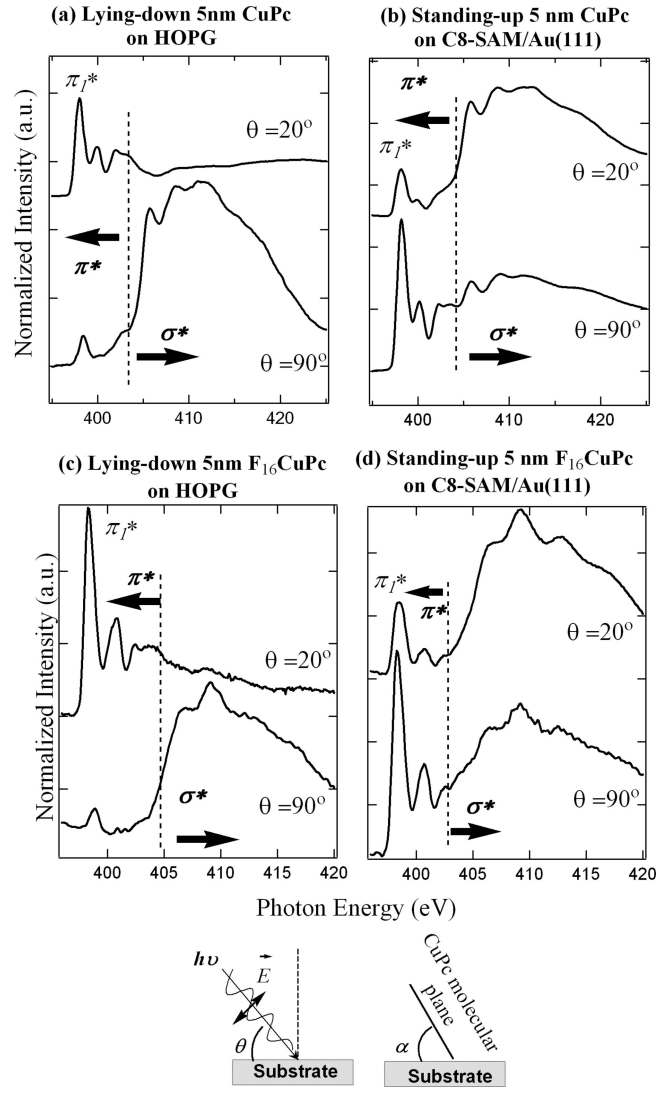

Figure 2. Angle-dependent NEXAFS spectra for the 5 nm CuPc on (a) HOPG and (b) C_8−SAM/Au(111) substrates, and 5 nm F_{16}CuPc on (c) HOPG and (d) C8-SAM/Au(111).

Experimental Section

PES and NEXAFS measurements were carried out at the Surface, Interface and Nanostructure Science (SINS) beamline of the Singapore Synchrotron Light Source.[32] The sample vacuum level shift was determined from PES spectra at the low-kinetic energy onset (secondary electron cutoff) using a photon energy of 60 eV

(17) Papageorgiou, N.; Salomon, E.; Angot, T.; Layet, J.-M.; Giovanelli, L.; Lay, G. L. *Prog. Surf. Sci.* **2004**, *77*, 139.
(18) Chen, W.; Huang, H.; Wee, A. T. S. *Chem. Commun.* **2008**, 4276.
(19) (a) Kraft, A.; Temirov, R.; Henze, S. K. M.; Soubatch, S.; Rohlfing, M.; Tautz, F. S. *Phys. Rev. B.* **2006**, *74*, 041402. (b) Temirov, R.; Soubatch, S.; Luican, A.; Tautz, F. S. *Nature* **2006**, *444*, 350. (c) Hauschild, A.; Karki, K.; Cowie, B. C. C.; Rohlfing, M.; Tautz, F. S.; Sokolowski, M. *Phys. Rev. Lett.* **2005**, *94*, 036106. (d) Eremtchenko, M.; Schaefer, J. A.; Tautz, F. S. *Nature* **2003**, *425*, 602.
(20) Loi, M. A.; Da Como, E.; Dinelli, F.; Murgia, M.; Zamboni, R.; Biscarini, F.; Muccini, M. *Nat. Mater.* **2005**, *4*, 81.
(21) Kowarik, S.; Gerlach, A.; Sellner, S.; Schreiber, F.; Cavalcanti, L.; Konovalov, O. *Phys. Rev. Lett.* **2006**, *96*, 125504.
(22) Peisert, H.; Schwieger, T.; Auerhammer, J. M.; Knupfer, M.; Golden, M. S.; Fink, J.; Bressler, P. R.; Mast, M. *J. Appl. Phys.* **2001**, *90*, 466.
(23) Fritz, S. E.; Martin, S. M.; Frisbie, C. D.; Ward, M. D.; Toney, M. F. *J. Am. Chem. Soc.* **2004**, *126*, 4084.
(24) de Oteyza, D. G.; Barrena, E.; Ossó, J. O.; Sellner, S.; Dosch, H. *J. Am. Chem. Soc.* **2006**, *128*, 15052.
(25) Dholakia, G. R.; Meyyappan, M.; Facchetti, A.; Marks, T. J. *Nano Lett.* **2006**, *6*, 2447.
(26) Thayer, G. E.; Sadowski, J. T.; zu Heringdorf, F. M.; Sakurai, T.; Tromp, R. M. *Phys. Rev. Lett.* **2005**, *95*, 256106.
(27) (a) Chen, W.; Zhang, H. L.; Huang, H.; Chen, L.; Wee, A. T. S. *Appl. Phys. Lett.* **2008**, *92*, 193301. (b) Chen, W.; Zhang, H. L.; Huang, H.; Chen, L.; Wee, A. T. S. *ACS Nano* **2008**, *2*, 693.
(28) (a) Chen, W.; Huang, H.; Chen, S.; Chen, L.; Zhang, H. L.; Gao, X. Y.; Wee, A. T. S. *Appl. Phys. Lett.* **2007**, *91*, 114102. (b) Chen, W.; Chen, S.; Huang, H.; Qi, D. C.; Gao, X. Y.; Wee, A. T. S. *Appl. Phys. Lett.* **2008**, *92*, 063308. (c) Chen, W.; Huang, H.; Chen, S.; Chen, L.; Zhang, H. L.; Gao, X. Y.; Wee, A. T. S. *J. Phys. Chem. C* **2008**, *112*, 5036.
(29) Chen, W.; Wang, L.; Qi, D. C.; Chen, S.; Gao, X. Y.; Wee, A. T. S. *Appl. Phys. Lett.* **2006**, *88*, 184102.
(30) (a) Chen, W.; Huang, C.; Gao, X. Y.; Wang, L.; Zhen, C. G.; Qi, D. C.; Chen, S.; Zhang, H. L.; Loh, K. P.; Chen, Z. K.; Wee, W. T. S. *J. Phys. Chem. B.* **2006**, *110*, 26075. (b) Chen, W.; Chen, S.; Qi, D. C.; Gao, X. Y.; Chen, Z. K.; Wee, W. T. S. *Adv. Funct. Mater.* **2007**, *17*, 1339.
(31) (a) Wang, J.; Wang, H. B.; Yan, X. J.; Huang, H. C.; Yan, D. H. *Appl. Phys. Lett.* **2005**, *87*, 093507. (b) Wang, J.; Wang, H. B.; Yan, X. J.; Huang, H. C.; Jin, D.; Shi, J. W.; Tang, Y. H.; Yan, D. H, *Adv. Funct. Mater.* **2006**, *16*, 824. (c) Lau, K. M.; Tang, J. X.; Sun, H. Y.; Lee, C. S.; Lee, S. T.; Yan, D. H. *Appl. Phys. Lett.* **2006**, *88*, 173513.

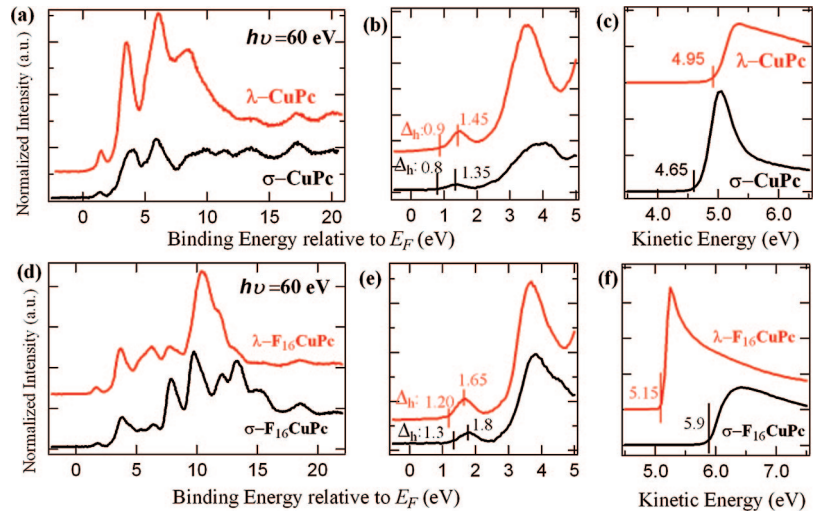

Figure 3. Synchrotron PES spectra for lying-down CuPc and F_{16}CuPc on HOPG and standing-up CuPc and F_{16}CuPc on C8-SAM/Au(111): (a, d) valence band spectra at the low-binding energy part and (b, e) corresponding near the E_F region spectra from panel a and d, and (c, f) PES spectra at the low-kinetic energy part (secondary electron cutoff). All spectra are measured with photon energy of 60 eV. All binding energy are relative to the Fermi level position of the electron analyzer. λ represents the lying-down molecular configuration and σ the standing-up configuration.

Table 1. Summary of Sample Parameters: Hole Injection Barriers (Δ_h), Work Functions (ϕ), Ionization Potential (IP = $\Delta_h+\phi$), and Tilt Angle α of the Molecular Plane with Respect to the Substrate Surface (obtained from NEXAFS results)[a]

	Δ_h (eV)	ϕ (eV)	IP (eV)	α
5 nm λ-CuPc on HOPG	0.90	4.25	5.15	20°
5 nm σ-CuPc on C8-SAM	0.80	3.95	4.75	75°
5 nm λ-F_{16}CuPc on HOPG	1.20	4.45	5.65	15°
5 nm σ-F_{16}CuPc on C8-SAM	1.30	5.20	6.50	70°

[a] The error bar for PES results (Δ_h, ϕ, and IP) and α are ± 0.05 eV and ± 5°, respectively. λ represents the lying-down molecular configuration and σ the standing-up configuration.

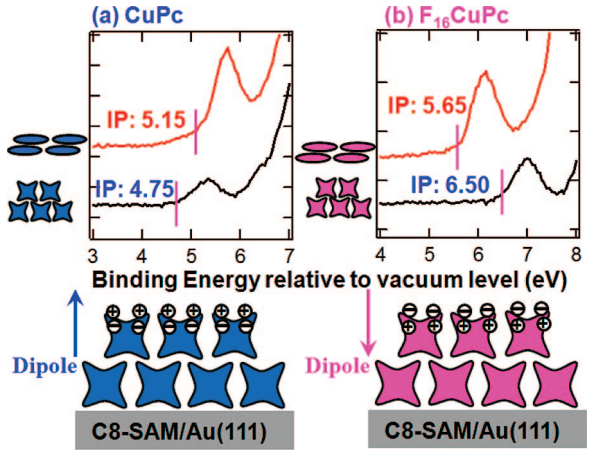

Figure 4. Synchrotron PES valence band spectra for lying-down and standing-up thin films of (a) CuPc and (b) F_{16}CuPc. All binding energies are relative to the vacuum level. The cartoons below show oppositely oriented surface dipoles (originating from different intramolecular dipolar bonds exposed at the surfaces) induced in the standing-up CuPc and F_{16}CuPc thin films.

with negative 5 V sample bias. The sample work function ϕ was obtained through the equation $\phi = h\upsilon - W$, where W is the spectrum width (the energy difference between the substrate Fermi level and low kinetic energy onset).[16] The ϕ of the electron analyzer was measured to be 4.30 ± 0.05 eV. The NEXAFS measurements were performed in total-electron yield (TEY) mode with a photon energy resolution of 0.1 eV. The linear polarization factor of synchrotron light at the SINS beamline was measured to be about 0.95. All the PES and NEXAFS measurements were performed at room temperature (RT).

Monolayers of octane-1-thiol (C_8−SAM) (Sigma-Aldrich) were formed by spontaneous adsorption on Au(111)/mica substrates (SPI, USA). In all cases the Au(111)/mica samples were immersed in 3 mL of 1 mM solutions in an N_2 environment for 48 h, using distilled ethanol as the solvent.[33] After growth, the samples were thoroughly rinsed using ethanol and immediately transferred into the UHV chamber of the SINS beamline. Fresh-cleaved highly ordered pyrolytic graphite (HOPG) substrates were thoroughly degassed in the UHV chamber at around 500 °C overnight before deposition. For NEXAFS and PES experiments, F_{16}CuPc (Sigma-Aldrich, 85%) and CuPc (Sigma-Aldrich, sublimation grade, 99.9%) were deposited in situ from K-cells onto HOPG and C_8−SAM/Au(111) substrates at RT in the main chamber of the SINS beamline (base pressure better than 6×10^{-11} mbar). Prior to deposition, F_{16}CuPc was purified twice by gradient vacuum sublimation (Creaphys, Germany). Deposition rates of 0.2 nm/min for CuPc and 0.1 nm/min for F_{16}CuPc were chosen in our NEXAFS and PES experiments. The deposition rates for both molecules were precalibrated by a quartz-crystal-microbalance (QCM) under similar growth conditions. The actual deposition rates were further calibrated by monitoring the attenuation in intensity of the Au $4f_{7/2}$ peak before and after the deposition on a sputter-cleaned poly Au sample.[34]

Results and Discussion

The molecular structures of CuPc and F_{16}CuPc are shown by schematic drawings a and b in Figure 1, respectively. Both molecules are planar with four peripheral benzene rings terminated by either 16 H atoms for CuPc or 16 F atoms for F_{16}CuPc. The molecular orientations of thick films of CuPc and F_{16}CuPc on HOPG and C8-SAM-terminated Au(111)

(32) (a) Chen, W.; Xu, H.; Liu, L.; Gao, X. Y.; Qi, D. C.; Peng, G. W.; Tan, S. C.; Feng, Y. P.; Loh, K. P.; Wee, A. T. S. *Surf. Sci.* **2005**, *596*, 176. (b) Chen, W.; Chen, S.; Qi, D. C.; Gao, X. Y.; Wee, A. T. S. *J. Am. Chem. Soc.* **2007**, *129*, 10418. (c) Yu, X. J.; Wilhelmi, O.; Moser, H. O.; Vidyaraj, S. V.; Gao, X. Y.; Wee, A. T. S.; Nyunt, T.; Qian, H. J.; Zheng, H. W. *J. Electron Spectrosc. Relat. Phenom.* **2005**, *144*, 1031.
(33) Chen, W.; Wang, L.; Huang, C.; Lin, T. T.; Gao, X. Y.; Loh, K. P.; Chen, Z. K.; Wee, A. T. S. *J. Am. Chem. Soc.* **2006**, *128*, 935.
(34) Seah, M. P.; Dench, W. A. *Surf. Interface Anal.* **1979**, *1*, 2.

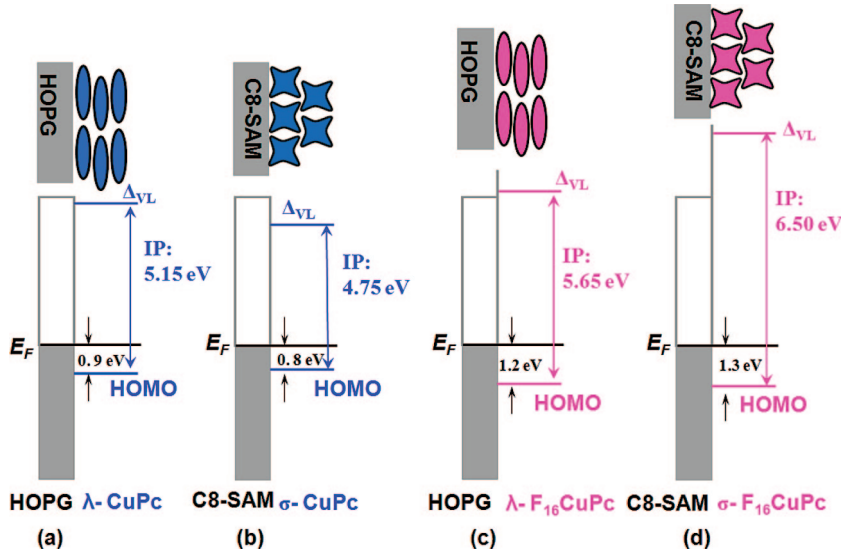

Figure 5. Schematics for the energy level diagrams of (a) λ-CuPc on HOPG, (b) σ-CuPc on C8-SAM, (c) λ-F_{16}CuPc on HOPG, and (d) σ-F_{16}CuPc on C8-SAM.

are confirmed by in situ NEXAFS measurements. NEXAFS was used to monitor the resonance from the core level of a specific atomic species of a molecule (for example, the 1s core level of nitrogen atoms in a molecule) to its unoccupied molecular orbitals (π^* and σ^* orbitals).[35] In principle, the resonance to the unoccupied π^* or σ^* orbital is strong when the electronic field vector **E** of the incident linear polarized synchrotron light has a large projection along the direction of the π^* or σ^* orbital, and vanishes when **E** is perpendicular to the π^* or σ^* orbital.[35] For the planar CuPc and F_{16}CuPc molecules, the σ^* and π^* orbitals are directed essentially in-plane and out-of-plane, respectively. Therefore, angle-dependent NEXAFS can be used to probe the molecular orientations in CuPc and F_{16}CuPc thin films. Panels a and b in Figure 2 show the angle-dependent NEXAFS spectra of 5 nm CuPc on HOPG and C8-SAM-terminated Au(111), respectively. As shown in Figure 2a, the first three sharp absorption peaks (397−404 eV) are assigned to the excitations from N 1s core level to individual π^* states, and the broad absorption peaks (404 − 415 eV) at higher photon energies to transitions to the σ^* states.[28−30] The π^* resonances of CuPc are greatly enhanced at grazing incidence and depressed at normal incidence. As such, the angular-dependence of NEXAFS spectra in Figure 2a confirms that CuPc molecules lie flat on HOPG. To simplify the estimation of molecular tilt angle using NEXAFS, we approximate the synchrotron light linear polarization factor of 0.95 to be 1. As such, the intensity I of the π_1^* resonance is related to the tilt angle α of the CuPc molecular plane with respect to the substrate plane and the synchrotron light incidence angle θ by[35]

$$I(\theta) \propto 1 + \frac{1}{2}(3\cos^2\theta - 1)(3\cos^2\alpha - 1)$$

Using the intensity ratio $R(\pi_1^*) = I(90°)/I(20°)$, we estimate the average tilt angle α for 5 nm CuPc on HOPG to be 20° ± 5°. As shown in Figure 2(b), the angle-dependence of NEXAFS spectra for 5 nm CuPc on C8-SAM terminated Au(111) is reversed, i.e., the π^* resonances are greatly enhanced at normal incidence and depressed at grazing incidence. This suggests that CuPc molecules stand upright on C8-SAM-terminated Au(111) with average tilt angle α of 75° ± 5°. Similar orientation dependence of 5 nm F_{16}CuPc thin films are obtained; they lie flat on HOPG with average tilt angle α of 15° ± 5° (Figure 2c) and stand up on C8-SAM-terminated Au(111) with average tilt angle α of 70° ± 5° (Figure 2d).

The orientation-dependent energy level alignment of both standing-up and lying-down CuPc and F_{16}CuPc thin films has been investigated by *in* situ high-resolution PES. Figure 3 shows the PES valence band (VB) spectra at the low-binding energy region (Figure 3a, b, d, e), and spectra at the low-kinetic energy region (Figure 3c, f). The hole injection barriers (Δ_h) can be measured from the energy difference between the substrate Fermi level and the HOMO leading edge (linear extrapolation of the low-binding energy onset).[16] The E_{vac} or ϕ values were measured with −5 V sample bias by linear extrapolation of the low-kinetic energy onset (secondary electron cutoff) of PES spectra. The IP equals to the sum of Δ_h and ϕ. These values are summarized in Table 1 for different films. As shown in panels a and d in Figure 3, the PES spectra show the apparent angle dependence of the valence band features for both CuPc and F_{16}CuPc films. In particular, the E_{vac} or ϕ of the standing up CuPc is 0.30 ± 0.05 eV lower than that of the lying-down film; while the E_{vac} or ϕ of the standing up F_{16}CuPc is 0.75 ± 0.05 eV higher than that of the lying-down film. However, Δ_h does not show strong angle dependence for both CuPc and F_{16}CuPc films.

Panels a and b in Figure 4 show the replotted valence band PES spectra relative to the vacuum level for both lying-down and standing-up thin films of CuPc and F_{16}CuPc, respectively. The linear extrapolation of the low-binding energy onset corresponds to the IP of the films, which are highlighted in the Figure 4. It clearly reveals opposite orientation-dependence of IP for CuPc and F_{16}CuPc thin films, i.e., the IP of the standing up CuPc is 0.40 ± 0.05 eV lower than that of the lying-down film; while the IP of the standing up

(35) Stöhr, J. *NEXAFS Spectroscopy*; Springer-Verlag: Berlin, 1992.

F_{16}CuPc is 0.85 ± 0.05 eV higher than that of the lying-down film. We attribute the observed orientation-dependent IP to the opposite oriented surface dipoles induced in the well-ordered standing-up CuPc and F_{16}CuPc thin films, as shown by the cartoon below Figure 4(a) and 4(b). The opposite surface dipoles originate from the different intramolecular dipolar bonds exposed at the surfaces of the standing-up CuPc and F_{16}CuPc thin films, i.e., a upward pointing surface dipole for the standing-up CuPc thin film and a downward pointing surface dipole for the standing-up F_{16}CuPc thin film because of the different bond polarities of C−H and C−F bonds. Our results are consistent with a recent paper by Salzmann et al., reporting a very similar orientation dependent IP for both standing-up and lying-down pentacene and perfluoro-pentacene thin films.[14] Figure 5 displays the energy level diagrams for the both standing-up and lying-down CuPc and F_{16}CuPc thin films, clearly showing the orientation-dependent IPs.

Conclusion

In summary, using model systems of both standing-up and lying-down CuPc and F_{16}CuPc thin films, we clearly demonstrate the orientation dependent IPs of organic thin films by synchrotron-based high-resolution PES and NEXAFS measurements, in consistent with previous reports.[8,14] It is found that the IP for the standing-up CuPc thin film (IP = 4.75 eV) is 0.40 eV lower than that of the lying-down film (IP = 5.15 eV); while the IP of the standing up F_{16}CuPc (IP = 6.50 eV) is 0.85 eV higher than that of the lying-down film (IP = 5.65 eV). The observed reversed orientation dependence in the IPs for CuPc and F16CuPc thin films can be explained by the opposite intrinsic surface dipoles induced in the standing-up CuPc and F_{16}CuPc molecular layers, which originate from the different intramolecular dipolar bonds exposed at the surfaces, i.e., the different bond polarities of C−H and C−F bonds. Our results suggest that it is not applicable to estimate the energy level alignments by simply using a universal value of IPs for highly crystalline organic thin films or organic single crystal- based organic electronic devices.[8] In particular, in designing the organic p−n heterojunction-based photovoltaic cells with appropriate energy-level offsets (open circuit voltage) or tuning the charge injection barriers in organic light-emitting diodes, the orientation-dependent IPs for molecules in ordered assemblies must be taken into account.

Acknowledgment. W.C. acknowledges the financial support by LKY PDF fellowship. The authors thank J. Ma and S. Chen for helpful discussions. The authors acknowledge the support from the A*STAR Grant R-398-000-036-305 and ARF Grant R-144-000-196-112.

CM8016352